Femtosecond luminescence spectroscopy of core states in silicon nanocrystals

Žídek, K.; Trojánek, F.; Malý, P.; Ondič, L.; Pelant, I.; Dohnalová, K.; Šiller, L.; Little, R.; Horrocks, B.R.

DOI
10.1364/OE.18.025241

Publication date
2010

Document Version
Final published version

Published in
Optics Express

Femtosecond luminescence spectroscopy of core states in silicon nanocrystals

K. Žídek,[1,2,*] F. Trojánek,[1] P. Malý,[1] L. Ondič,[1,2] I. Pelant,[2] K. Dohnalová,[2,3] L. Šiller,[4] R. Little,[4] and B. R. Horrocks[5]

[1]*Faculty of Mathematics and Physics, Charles University in Prague, Ke Karlovu 3, 121 16 Prague, Czech Republic*
[2]*Institute of Physics, Academy of Sciences of the Czech Republic, v.v.i., Cukrovarnická 10, 162 53 Prague, Czech Republic*
[3]*Van der Waals-Zeeman Institute, University of Amsterdam, 65 Vackenierstraat, NL-1018 XE Amsterdam, Netherlands*
[4]*School of Chemical Engineering and Advanced Materials, Newcastle University, Newcastle upon Tyne, NE1 7RU, UK*
[5]*School of Chemistry, Newcastle University, Newcastle upon Tyne, NE1 7RU, UK*
**zidek@karlov.mff.cuni.cz*

Abstract: We present a study of ultrafast carrier transfer from highly luminescent states inside the core of silicon nanocrystal (due to quasidirect transitions) to states on the nanocrystal-matrix interface. This transfer leads to a sub-picosecond luminescence decay, which is followed by a slower decay component induced by carrier relaxation to lower interface states. We investigate the luminescence dynamics for two different surface passivation types and we propose a general model describing spectral dependence of ultrafast carrier dynamics. Our results stress the crucial role of the energy distribution of the interface states on surface-related quenching of quasidirect luminescence in silicon nanocrystals. We discuss how to avoid this quenching in order to bring the attractive properties of the quasidirect recombination closer to exploitation.

OCIS codes: (300.6530) Spectroscopy, ultrafast; (300.6280) Spectroscopy, fluorescence and luminescence; (310.6628) Subwavelength structures, nanostructures; (160.6000) Semiconductor materials.

References and links

1. A. G. Cullis, and L. T. Canham, "Visible light emission due to quantum size effects in highly porous crystalline silicon," Nature **353**(6342), 335–338 (1991).
2. S. Ossicini, L. Pavesi, and F. Priolo, *Light Emitting Silicon for Microphotonics*, Springer Tracts in Modern Physics 194 (Springer-Verlag, Berlin, 2003).
3. L. Khriachtchev, *Silicon Nanophotonics: Basic Principles, Present Status and Perspectives* (World Scientific, Singapore, 2008).
4. N. H. Alsharif, C. E. M. Berger, S. S. Varanasi, Y. Chao, B. R. Horrocks, and H. K. Datta, "Alkyl-capped silicon nanocrystals lack cytotoxicity and have enhanced intracellular accumulation in malignant cells via cholesterol-dependent endocytosis," Small **5**(2), 221–228 (2009).
5. D. Kovalev, H. Heckler, M. Ben-Chorin, G. Polisski, M. Schwartzkopff, and F. Koch, "Breakdown of the k-conservation rule in Si nanocrystals," Phys. Rev. Lett. **81**(13), 2803–2806 (1998).
6. M. S. Hybertsen, "Absorption and emission of light in nanoscale silicon structures," Phys. Rev. Lett. **72**(10), 1514–1517 (1994).
7. N. Holonyak, J. C. Campbell, M. H. Lee, J. T. Verdeyen, W. L. Johnson, M. G. Craford, and D. Finn, "Pumping of $GaAs_{1-x}P_x$: N (at 77 °K, for x≤0.53) by an electron beam from a gas plasma," J. Appl. Phys. **44**(12), 5517–5521 (1973).
8. M. V. Wolkin, J. Jorne, P. M. Fauchet, G. Allan, and C. Delerue, "Electronic States and Luminescence in Porous Silicon Quantum Dots: The Role of Oxygen," Phys. Rev. Lett. **82**(1), 197–200 (1999).
9. F. Trojánek, K. Neudert, P. Malý, K. Dohnalová, and I. Pelant, "Ultrafast photoluminescence in silicon nanocrystals studied by femtosecond up-conversion technique," J. Appl. Phys. **99**(11), 116108 (2006).
10. A. Othonos, E. Lioudakis, and A. G. Nassiopoulou, "Surface-Related States in Oxidized Silicon Nanocrystals Enhance Carrier Relaxation and Inhibit Auger Recombination," Nanoscale Res. Lett. **3**(9), 315–320 (2008).
11. V. I. Klimov, J. C. Schwarz, D. McBranch, and C. W. White, "Initial carrier relaxation dynamics in ion-implanted Si nanocrystals: Femtosecond transient absorption study," Appl. Phys. Lett. **73**(18), 2603 (1998).

#136645 - $15.00 USD Received 15 Oct 2010; revised 4 Nov 2010; accepted 9 Nov 2010; published 17 Nov 2010

12. L. Van Dao, J. Davis, P. Hannaford, Y.-H. Cho, M. A. Green, and E.-C. Cho, "Ultrafast carrier dynamics of Si quantum dots embedded in SiN matrix," Appl. Phys. Lett. **90**(8), 081105 (2007).
13. W. de Boer, H. Zhang, and T. Gregorkiewicz, "Optical spectroscopy of carrier relaxation processes in Si nanocrystals," Mater. Sci. Eng. B **159–160**, 190–193 (2009).
14. G. Juška, A. Medvids, and V. Gulbinas, "Initial charge carrier dynamics in porous silicon revealed by time-resolved fluorescence and transient reflectivity," Phys. Sta. Solidi A **207**, 188–193 (2010).
15. F. Trojánek, K. Neudert, K. Žídek, K. Dohnalová, I. Pelant, and P. Malý, "Femtosecond photoluminescence spectroscopy of silicon nanocrystals," Phys. Stat. Solidi C **3**(11), 3873–3876 (2006).
16. M. Sykora, L. Mangolini, R. D. Schaller, U. Kortshagen, D. Jurbergs, and V. I. Klimov, "Size-dependent intrinsic radiative decay rates of silicon nanocrystals at large confinement energies," Phys. Rev. Lett. **100**(6), 067401 (2008).
17. F. M. Dickinson, T. A. Alsop, N. Al-Sharif, C. E. M. Berger, H. K. Datta, L. Šiller, Y. Chao, E. M. Tuite, A. Houlton, and B. R. Horrocks, "Dispersions of alkyl-capped silicon nanocrystals in aqueous media: photoluminescence and ageing," Analyst (Lond.) **133**(11), 1573–1580 (2008).
18. Y. Chao, L. Šiller, S. Krishnamurthy, P. R. Coxon, U. Bangert, M. Gass, L. Kjeldgaard, S. N. Patole, L. H. Lie, N. O'Farrell, T. A. Alsop, A. Houlton, and B. R. Horrocks, "Evaporation and deposition of alkyl-capped silicon nanocrystals in ultrahigh vacuum," Nat. Nanotechnol. **2**(8), 486–489 (2007).
19. L. Šiller, S. Krishnamurthy, L. Kjeldgaard, B. R. Horrocks, Y. Chao, A. Houlton, A. K. Chakraborty, and M. R. C. Hunt, "Core and valence exciton formation in x-ray absorption, x-ray emission and x-ray excited optical luminescence from passivated Si nanocrystals at the Si $L_{2,3}$ edge," J. Phys. Condens. Matter **21**(9), 095005 (2009).
20. R. J. Roston, B. R. Horrocks, and G. Roberts, "Distributed luminescence from alkyl-capped silicon quantum dots," J. Appl. Phys. **105**(9), 094302 (2009).
21. K. Dohnalová, L. Ondič, K. Kůsová, I. Pelant, J. L. Rehspringer, and R. R. Mafouana, "White-emitting oxide silicon nanocrystals: Discontinuity in spectral development with reducing size," J. Appl. Phys. **107**(5), 053102 (2010).
22. K. Dohnalová, I. Pelant, K. Kůsová, P. Gilliot, M. Galart, O. Crégut, J. L. Rehspringer, B. Hönerlage, T. Ostatnický, and S. Bakardjieva, "Closely packed luminescent silicon nanocrystals in a distributed-feedback laser cavity," N. J. Phys. **10**(6), 063014 (2008).
23. J. Valenta, A. Fučíková, I. Pelant, K. Kůsová, K. Dohnalová, A. Aleknavičius, O. Cibulka, A. Fojtík, and G. Kada, "On the origin of the fast photoluminescence band in small silicon nanoparticles," N. J. Phys. **10**(7), 073022 (2008).
24. J. Valenta, A. Fučíková, F. Vácha, F. Adamec, J. Humpolíčková, M. Hof, I. Pelant, K. Kůsová, K. Dohnalová, and J. Linnros, "Light-Emission Performance of Silicon Nanocrystals Deduced from Single Quantum Dot Spectroscopy," Adv. Funct. Mater. **18**(18), 2666–2672 (2008).
25. J. Shah, "Ultrafast Luminescence Spectroscopy Using Sum Frequency Generation," IEEE J. Quantum Electron. **24**(2), 276–288 (1988).
26. D. M. Mittleman, R. W. Schoenlein, J. J. Shiang, V. L. Colvin, A. P. Alivisatos, and C. V. Shank, "Quantum size dependence of femtosecond electronic dephasing and vibrational dynamics in CdSe nanocrystals," Phys. Rev. B Condens. Matter **49**(20), 14435–14447 (1994).
27. M. D. Garrett, M. J. Bowers, J. R. McBride, R. L. Orndorff, S. J. Pennycook, and S. J. Rosenthal, "Band edge dynamics in CdSe nanocrystals observed by ultrafast fluorescence upconversion," J. Phys. Chem. C **112**(2), 436–442 (2008).
28. K. Kůsová, O. Cibulka, K. Dohnalová, I. Pelant, J. Valenta, A. Fucíková, K. Zídek, J. Lang, J. Englich, P. Matějka, P. Stepánek, and S. Bakardjieva, "Brightly luminescent organically capped silicon nanocrystals fabricated at room temperature and atmospheric pressure," ACS Nano **4**(8), 4495–4504 (2010).

1. Introduction

Interest in the optical properties of silicon nanocrystals (Si NCs) grew rapidly following the discovery of efficient visible luminescence in porous silicon by Canham [1]. One of the main ideas behind this effort is to develop small and robust light source for the so-called silicon photonics, which would be compatible with existing silicon technology [2]. Furthermore, light-emitting Si NCs could be utilized also for optical sensing [3], waveguiding [3], as non-toxic fluorescent labels in living cells [4], etc.

One of specific and attractive features of nanometer-sized Si NCs is the occurrence of the so-called "quasidirect" electron-hole recombination [5,6]. Bulk silicon is a poor light emitter, because of its indirect bandgap. Radiative electron-hole recombination is inefficient since three quasiparticles (an electron, a hole and a phonon) have to take part to satisfy the conservation of momentum. On the other hand, in nanometer-sized Si NCs the severe carrier localization in the NC core entails strong delocalization of the carrier wavefunction in momentum space, which makes the no-phonon (i.e. quasidirect) radiative recombination possible. The concept is analogous to the case of isoelectronic impurities in bulk indirect semiconductors [7]. Such transitions are of great interest from the viewpoint of

#136645 - $15.00 USD Received 15 Oct 2010; revised 4 Nov 2010; accepted 9 Nov 2010; published 17 Nov 2010

photoluminescence (PL) efficiency, because they can put Si NCs on a par with direct bandgap semiconductors.

Unfortunately, commonly used Si NC surface chemistries hinder exploitation of the quasidirect core-related transition, because the excited carriers are very rapidly trapped at energetically more favorable interface states (states in the NC-matrix interface region) [8], where afterwards the vast majority of carriers recombine relatively slowly, with a decay time of 10-100 μs [9]. Extreme rates of carrier trapping at interface states [9,10] even completely prevent the core PL from being observed in standard c.w. PL experiments. Moreover, neither the high-temporal-resolution pump-and-probe techniques for studying transient absorption and reflectance applied to Si NCs [10–14] are able to reveal the ultrafast core emission.

To study the temporal behavior of this short-lived PL, special experimental techniques are required. Hitherto, only a few papers can be found in the literature that report on time-resolved observations of the quasidirect PL and its quenching by ultrafast carrier trapping at surface states. Trojanek et al. were the first who reported on the sub-picosecond PL decay [9,15], which has subsequently been confirmed by Sykora et al. [16].

In this article we study in detail the spectral dependence of the ultrafast PL decay rates, which, to the best of our knowledge, has not been reported before. We investigate two samples of Si NCs with greatly different surface passivations and different mean sizes. We propose a model which links the observed decay rates with the energy distribution of the NC interface states and surface-area-to-volume ratio. We verify the validity of our model in two independent ways and conclude by discussing how to employ the core-related quasidirect transitions in a useful luminescence output.

2. Experimental

2.1 Investigated samples

We investigated two well-characterized samples of Si NCs fabricated by electrochemical etching under different conditions and moreover with different surface chemistries. This enabled us to investigate common properties of ultrafast dynamics in Si NCs with different surface passivations. Alkyl passivation of Si NCs is promising for bio applications [4,17], whereas SiO_2 passivation is a standard Si passivation method in optoelectronics.

A sample, which we denominate “ALS” (alkylated sample), was prepared by a short etch (5 minutes) at high current density (500 mA/cm^2). The electrolyte consisted of 48% HF(aq) mixed in 1:1 volume ratio with ethanol. The layer of porous silicon was then transformed into isolated undecyl-passivated nanocrystals (C_{11}-SiNCs) by the hydrosilation reaction in undecene/toluene [18]. The NC alkylation procedure and subsequent preparation of the colloidal dispersion (2 mg of Si NCs in 250 μl of dichloromethane) is described in detail in Ref [18]. Characterization of Si NCs prepared by this method by means of FTIR spectroscopy, x-ray scattering, absorption (XAS), diffraction (XRD), emission (XES) and photoelectron spectroscopy (XPS) as well as atomic force (AFM) and scanning tunneling microscopy (STEM) can be found in Ref [18,19]. Optical properties of the alkylated Si NCs have been investigated in detail [17,20] together with possible application of the alkylated NCs as fluorescent labels [4]

Another sample, hereafter denominated “OXS” (oxidized sample), was prepared via a long (120 minutes) etching by applying a low current density (1.6 mA/cm^2). The electrolyte comprised 50% HF(aq) in 4:10 volume ratio with ethanol. Long-term oxidation and ageing of the sample took place at ambient conditions for 1 month. The etched porous Si layers were eventually pulverized and 1.6 mg of the oxidized porous Si powder was dispersed into 200 μl of UV grade ethanol. The Si NCs prepared by the porous Si oxidation have been characterized by many methods (FTIR, Raman spectroscopy, AFM, high-resolution transmission electron microscopy) [21–23] and various optical properties have been already studied (single NC spectroscopy [24], time-resolved measurements [9,21], stimulated emission [22], etc.).

#136645 - $15.00 USD Received 15 Oct 2010; revised 4 Nov 2010; accepted 9 Nov 2010; published 17 Nov 2010

Using the procedures described above, we have achieved colloidal dispersions of Si NCs, as shown by number of methods: AFM [23] and high-resolution transmission electron microscope [22] for the OXS sample, STEM [18] and XRD [19] for the ALS sample. Mean NC diameters were estimated to lie between 2.2 - 2.6 nm by a variety of methods in the case of ALS [18], and around 3.5 nm in case of OXS [22]. Both samples show long-term stability of their optical properties. The PL dynamics measurements were repeated several times on the same samples and the PL photon energy of the measured dynamics has been chosen in random order to avoid the possibility of PL dynamics changes being confounded by effects arising from any sample transformation or damage by UV light.

2.2 Experimental setup

The ultrafast PL time evolution was measured by a non-linear optical gating method, namely by making use of the so-called up-conversion setup [25] described in detail in our previous articles [9,15]. We used a Ti:Sapphire laser (Tsunami, Spectra Physics) providing 80 fs pulses with 82 MHz repetition rate. Frequency doubled pulses at 405 nm excited the samples (energy per pulse ~1 nJ) and the emitted PL signal was optically gated by pulses on the fundamental wavelength 810 nm in a BBO crystal by a sum-frequency (SF) generation. The SF signal was selected by a monochromator and detected by a Hamamatsu photon counter. We measured PL dynamics by changing a delay between the excitation and the gating pulse by an optical delay line. FWHM of the temporal response function of the experimental setup was 280 fs, which is increased compared to gating pulse length (80 fs) owing to different group velocities of the up-converted signal, PL signal and gating pulse frequency in the BBO crystal [25]. The spectral dependence of the PL was measured by a simultaneous BBO crystal rotation (phase-matching condition) and monochromator setting (setup spectral resolution ~8 nm).

PL spectra on the microsecond time scale were taken under excitation by the third harmonic of an Nd:YAG laser (355 nm) with nanosecond pulses (7 ns pulse width, 10 Hz repetition rate). PL was detected by an Andor iCCD (intensified CCD) camera coupled to the Andor Shamrock imaging spectrograph. Time-integrated spectra were measured under cw excitation at 325 nm (He-Cd laser). PL was detected by a CCD (Larry, LOT-Oriel) mounted on an Oriel MS125 spectrograph. Extinction spectra were measured by a conventional spectrophotometer (Analytik Jena, Specord).

All spectra in this article were measured at room temperature and they were corrected for the spectral response of the experimental setup.

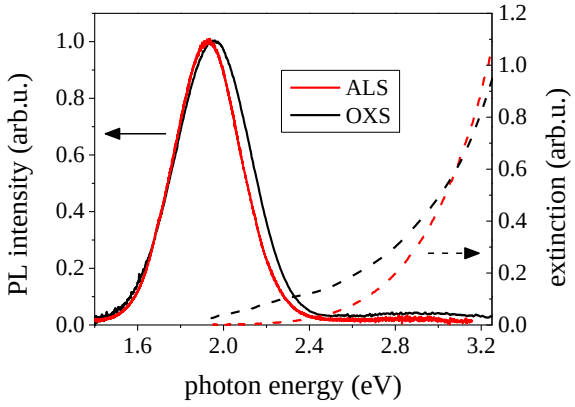

Fig. 1. Normalized time-integrated PL spectra excited by cw 325 nm (solid lines) and extinction (dashed lines) of ALS (red lines) and OXS (black lines) samples.

3. Results and discussion

In spite of very different preparation parameters, both samples reveal similar spectra of time-integrated PL and extinction (see Fig. 1). The extinction spectra show a rapid increase for

#136645 - $15.00 USD Received 15 Oct 2010; revised 4 Nov 2010; accepted 9 Nov 2010; published 17 Nov 2010

higher energies, typical of Si NCs. Due to the NC size distribution, discrete absorption bands (typical for e.g. II-VI semiconductor NCs) cannot be observed and the extinction spectra gradually increases from low-energy side, where also the absorption on the NC surface states can affect the spectrum. Time-integrated PL spectra consist in both cases of a dominant PL band in the red spectral region, which is usually attributed to the radiative recombination in NC interface states.

3.2 Ultrafast luminescence decay and spectra

Figure 2 displays ultrafast PL decay dynamics of the ALS sample for different PL photon energies together with a PL decay curve of the OXS sample (see inset in Fig. 2). The general characteristics of the decay are the same for both samples and all studied PL photon energies (1.8 eV to 2.5 eV). We observed a rapid onset of the PL, which we attribute to a fast relaxation of carriers inside NC. The ultrafast PL decay has a two-exponential character. Our previous results [9,15] and also those of other authors [10,16] suggest that the fast decay component is a consequence of the rapid carrier trapping into the interface states, leading to the spatial separation of carriers. The slow (picosecond) component of the ultrafast PL decay can be explained by the relaxation of the trapped carriers to lower interface states.

The proposed model is illustrated by a scheme in Fig. 2 (right hand side). Auger recombination can be excluded from the observed decay, because the decay dynamics are not affected by varying excitation power and, moreover, the average number of excited e-h pairs per NC is very low. Typical excitation fluence of 50 μJ/cm^2 corresponds to the photon flux of 10^{14} cm^{-2}. The concentration of NCs in the samples is in the order of 10^{17} cm^{-3} [22] (~2×10^{17} cm^{-3}), i.e. in a thin layer of 1 μm, where approx. 1% of the excitation photons is absorbed, the areal density of NCs reaches ~2×10^{13} cm^{-2}. Therefore we can roughly estimate that, on average, 0.05 e-h pairs are excited per NC.

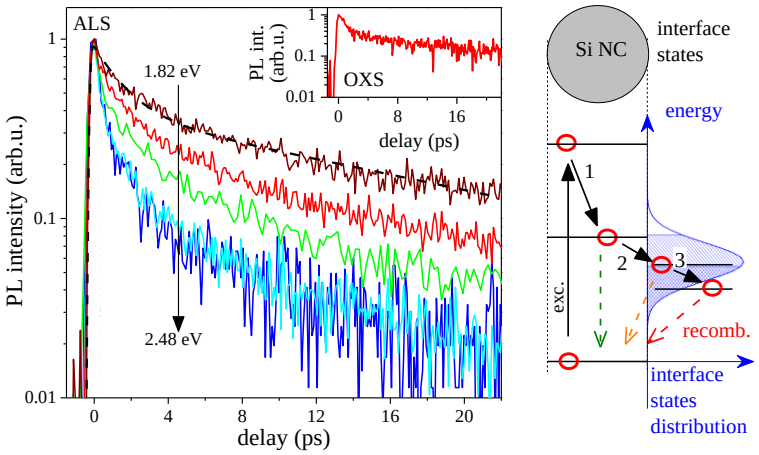

Fig. 2. Left: normalized ultrafast PL dynamics of the sample ALS (exc. 405 nm, 80 fs pulses) for various PL photon energy (solid lines), response function of the setup (dotted line), a two-exponential decay fit convoluted with the response function of the setup (dashed line); Inset: normalized ultrafast PL dynamics of the sample OXS (exc. 405 nm, 80 fs pulses, PL photon energy 1.96 eV); Right: scheme of the processes responsible for the ultrafast PL decay: 1) relaxation inside NC, 2) fast carrier trapping in interface states, 3) relaxation to lower interface states (see the text for details).

The decay curves in Fig. 2 show significant increase in the decay rate (i.e. decrease in the decay time) with increasing PL photon energy. To quantify these changes, we have fitted each curve by a two-exponential decay curve $I_{FAST}\exp(-k_{FAST}t)+I_{SLOW}\exp(-k_{SLOW}t)$ convoluted with a response function of the setup (a Gaussian function, FWHM 280 ps). The parameters k_{FAST} and k_{SLOW} stand for the decay rate of the fast and slow component respectively; I_{FAST} and

#136645 - $15.00 USD Received 15 Oct 2010; revised 4 Nov 2010; accepted 9 Nov 2010; published 17 Nov 2010

I_{SLOW} are the intensities of each component. It should be noted, that the two-exponential shape of the curve is only an approximation applicable for the initial part of the PL decay. The PL decay shape in later times is more complex, changing to a stretched-exponential decay on the microsecond time scale [9].

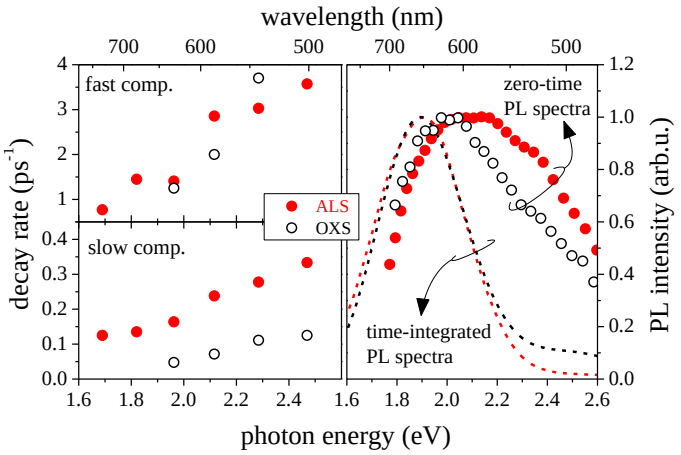

Fig. 3. Ultrafast PL dynamics spectral dependence of the ALS sample (red solid circles) and the OXS sample (black open circles) obtained by the PL dynamics two-exponential fitting (see the text for details); Left upper panel: fast component decay rate; Left lower panel: slow component decay rate; Right hand side: normalized zero-time PL spectra compared to the time-integrated PL spectra under the same excitation regime (exc. 405 nm, 80 fs pulses, ALS: red dashed line, OXS: black dashed line).

The spectral dependences of k_{FAST} and k_{SLOW} are shown in Fig. 3 (left hand side). Also here we observe an evident increase in the decay rate for higher PL photon energies. The right hand side of Fig. 3 displays PL spectra in the temporal maximum of PL dynamics (zero-time spectra) measured by the up-conversion technique compared to the time-integrated PL spectra under the same excitation regime (405 nm exc. wavelength, 80 fs pulse length, excitation fluence ~50 μJ/cm^2). Time-integrated PL spectra are red-shifted compared to the zero-time PL spectra as a consequence of carrier relaxation from core NC states to interface states.

It is worth noticing in Fig. 3 that, even if the time-integrated PL spectra of both the samples are very similar, the ALS sample zero-time emission is peaked at shorter wavelengths (~590 nm) in comparison with that of the OXS sample (~620 nm). This reflects stronger quantum confinement effect (larger gap opening) in the ALS sample that contains nanocrystals of smaller mean size (2.2 – 2.6 nm against 3.5 nm), and corroborates the assignment of the ultrafast PL to recombination involving in NC core states.

We have not discussed yet the possibility that carrier cooling inside NCs is responsible for the observed ultrafast PL decay. However, such an interpretation would be hardly tenable. First, even for photon energies as low as 1.8 eV, the PL rise time is well beyond the time resolution of the setup (280 fs) – see Fig. 2 and Fig. 4. This means that a very efficient carrier cooling mechanisms act on carriers already on a timescale much shorter than a typical time of the observed PL decay (up to 1 ps). Second, Sykora et al. [16] proved the presence of two light-emitting states (i.e. core and surface states) in the ultrafast PL evolution by observing the so-called “isostilbic point” in the normalized ultrafast PL spectra.

#136645 - $15.00 USD Received 15 Oct 2010; revised 4 Nov 2010; accepted 9 Nov 2010; published 17 Nov 2010

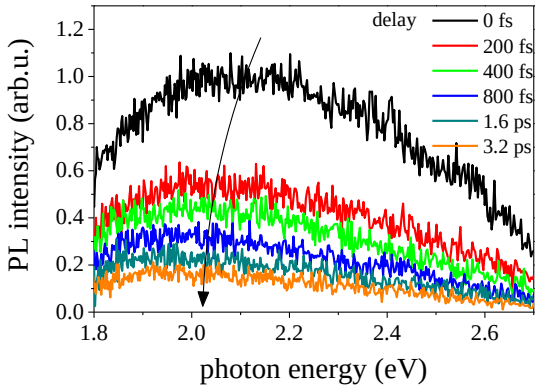

Fig. 4. Ultrafast PL spectra of sample ALS for various delays between excitation and gating pulse.

3.3 Model

We propose a simple model describing the observed spectral dependence of the ultrafast PL decay. We assume that the decay rates depend mainly on the two parameters: on a fraction of available traps with lower energy $N_{tr}(E)$ and on a surface-area-to-volume ratio (SA/V ratio) of the NC $\Theta(E)$. The quantity $N_{tr}(E)$ gives the fraction of states to which a carrier can relax from its actual energy level. The SA/V ratio $\Theta(E)$ accounts for the number of interface states proportional to the NC surface area together with an amplitude of the carrier wavefunction in the interface region [26,27]. As the SA/V ratio depends on the NC size, it also has a spectral dependence. Taking into account that the carrier trapping probability is proportional to both the number of available states and the SA/V ratio, we can express the decay rate k_{FAST} as

$$k_{FAST} \propto N_{tr}(E) \times \Theta(E). \quad (1)$$

On the other hand, a carrier already trapped in the surface state has a wavefunction distributed in the interface region independently of the NC size. Therefore, the relaxation rate k_{SLOW} depends only on the number of available traps with a lower energy, i.e.:

$$k_{SLOW} \propto N_{tr}(E). \quad (2)$$

From Eq. (1) and (2) it is obvious that a crucial role in ultrafast dynamics is played by the number of available traps (interface states), which varies for different NC passivations.

3.4 Interface states energy distribution

The interface states are also responsible for the PL emitted on long (microsecond) timescale. Therefore we can obtain information about energy distribution of interface states $\rho(E)$ from long-living PL spectra. Particularly, we measured spectrum of the PL emitted within the first microsecond after excitation.

The samples were excited by 355 nm nanosecond pulses to create e-h pairs energetically high above the bandgap. The time integration window (0-1 μs) was chosen to be long enough compared to excitation pulse length and at the same time short enough compared to typical lifetimes of the long-lived PL (21 μs for ALS [20], 5-10 μs for OXS [21]).

In order to match the PL spectrum to the spectral distribution of the interface states, one has to fill the states. We excited the samples by pulses up to a fluence of 20 mJ/cm^2, which generated several e-h pairs per NC. When increasing the intensity, we observed very slight shift in spectral PL position to higher energies, as one can see in Fig. 5. It can be attributed to trap states filling, which is very weak due to the high number of states. The spectral shift stops for high excitation fluences. We assume that traps are practically filled for such

#136645 - $15.00 USD Received 15 Oct 2010; revised 4 Nov 2010; accepted 9 Nov 2010; published 17 Nov 2010

intensities and the PL spectrum can be taken as the spectral distribution $\rho(E)$ of the interface traps.

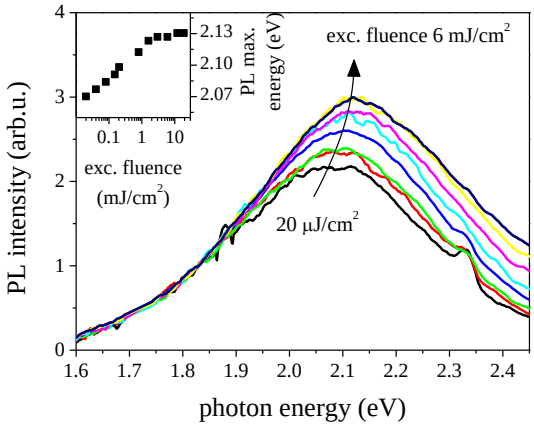

Fig. 5. PL spectra of the OXS sample under 355 nm excitation (Nd:YAG, 7 ns pulses) for various excitation intensity, normalized to the low-energy side of PL, inset: PL maximum position dependence on the excitation pulse energy.

The measured spectral distributions of traps $\rho(E)$ in both samples are shown in Fig. 6 a) (inset). We calculated the relative number of traps $N_{tr}(E)$ with energy lower than E by numerical integration of the distribution $\rho(E)$ from the lowest measured energy (1.5 eV) to energy E:

$$N_{tr}(E) \propto \int_{1.5\mathrm{eV}}^{E} \rho(\varepsilon)\, d\varepsilon. \tag{3}$$

3.5 Model verification and validation

The spectral dependence of $N_{tr}(E)$, which was extracted from PL emission spectra measurements, is shown in Fig. 6 a) (lines). To demonstrate the internal consistency of our approach, we also plot in Fig. 6 a) rates of the slow component of the relaxation dynamics $k_{SLOW}(E)$ extracted from the ultrafast PL dynamics measurements (symbols). According to Eq. (2), the curves $N_{tr}(E)$ and the relaxation rate $k_{SLOW}(E)$ in Fig. 6 a) should exhibit the same trend. Obviously, this is the case. One can see very good overall agreement after proper scaling and adding a constant to the $N_{tr}(E)$ curves: this is necessary because we know only the relative number of available traps and do not integrate from zero energy and therefore do not account for relaxation to some lower states.

We can proceed even further in exhibiting the self-consistency of our approach. Dividing Eq. (1) by Eq. (2) leads to an elimination of the N_{tr} spectral dependence and yields immediately

$$k_{FAST} / k_{SLOW} \propto \Theta(E), \tag{4}$$

i.e. the ratio k_{FAST}/k_{SLOW} should be proportional to SA/V ratio. The SA/V ratio affects the quenching of the initial PL emitted by a recombination of carriers in the NC core states. The energy of these states is determined by the NC size; therefore we can calculate for each PL photon energy the corresponding NC diameter by applying the experimental correlation of Wolkin et al. [8]. In Fig. 6 b) one can see the dependence of k_{FAST}/k_{SLOW} ratio on the NC size calculated from the PL dynamics. For both samples the data can be well fitted by the expected *1/d* dependence, where *d* stands for NC diameter.

#136645 - $15.00 USD Received 15 Oct 2010; revised 4 Nov 2010; accepted 9 Nov 2010; published 17 Nov 2010

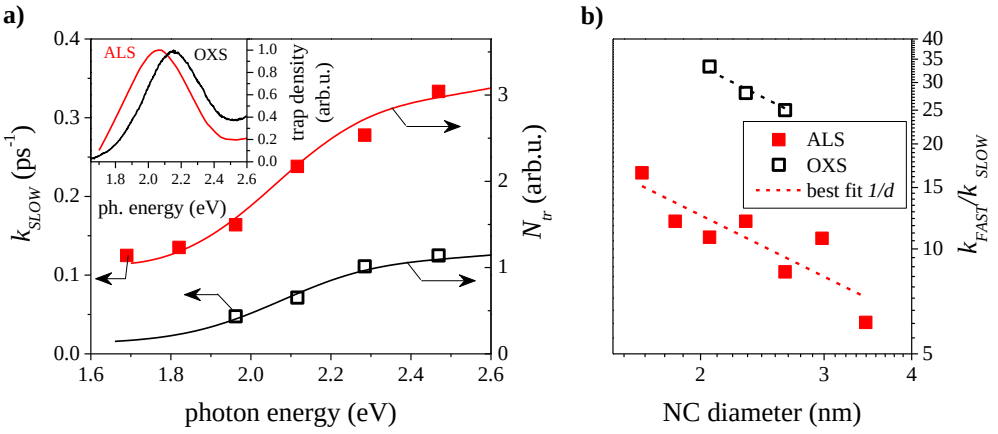

Fig. 6. a) Measured relaxation rates in the interface states for the OXS (black open squares) and ALS (red solid squares) samples, which are compared to fraction of traps with lower energy of the ALS (red line) and OXS (black line) samples; Inset: Spectral distribution of the trap number obtained from PL spectra (see text for details). b) Decay rates ratio k_{FAST}/k_{SLOW} dependence on NC diameter for the ALS and OXS sample with the best fit by *1/d* function (dashed lines).

Finally, one can see from the results that different passivation types of Si NCs lead to a two-exponential ultrafast PL decay with similar spectral dependence. This is consistent with the proposed model – changes in passivation can alter the interface states energy and the trapping rate, but the PL decay will keep the observed two-exponential character as a consequence of two processes being involved in initial carrier dynamics. Therefore the model implications are general for all Si NC surface states, independent of particular surface chemistry. Analogous processes lead to the two-exponential PL decay observed also for other semiconductor NCs, e.g. CdSe [27].

4. Conclusion

We have observed that the ultrafast dynamics of PL in Si NCs of diametrically different surface passivation types (silicon oxide and alkyl passivation) follow similar patterns. This, apart from other facts, confirms the origin of this PL in NC core states. Our measurements and proposed model indicate that the carriers are trapped extremely rapidly into the interface states and afterwards they relax to lower surrounding states. The key role in PL decay dynamics is played by energy distribution of the interface states and the SA/V ratio of NCs.

Our results strongly suggest that obtaining an efficient quasi-direct PL recombination from sufficiently small Si NCs is possible only by preventing photocarrier trapping in the low-energy states surrounding NC and, instead, by “forcing” them thereby to remain in the NC core. There are indications that a suitable surface capping may exist: we have reported recently on original way of photochemical passivation of Si NCs, in which the slow (microsecond) PL component, typical for the NC surface states recombination, is entirely lacking and these Si NCs emit an efficient PL with a short radiative lifetime of 10 ns [28]. Further research in this direction is indispensable, anyhow.

Acknowledgments

We gratefully acknowledge financial support of the Ministry of Education of the Czech Republic (center LC 510, research plan MSM0021620834), the Charles University in Prague (GA UK project No. 17808 and 73910; SVV-2010-26130), GAAV (Grant No. IAA101120804), the institutional Research Plan AV0Z 10100521 and KAN (Grant. No. 400100701). BRH and LŠ would like to thank EPSRC and ONE for funding work in Si NCs.

#136645 - $15.00 USD Received 15 Oct 2010; revised 4 Nov 2010; accepted 9 Nov 2010; published 17 Nov 2010